

# Quenching across quantum critical points: role of topological patterns

DIPTIMAN SEN<sup>1</sup> and SMITHA VISHVESHWARA<sup>2</sup>

<sup>1</sup> *Centre for High Energy Physics, Indian Institute of Science, Bangalore 560012, India*

<sup>2</sup> *Department of Physics, University of Illinois at Urbana-Champaign, 1110 W. Green St, Urbana, IL 61801, USA*

PACS 64.70.Tg – Quantum phase transitions

PACS 75.10.Jm – Quantized spin models

**Abstract.** - We introduce a one-dimensional version of the Kitaev model consisting of spins on a two-legged ladder and characterized by  $Z_2$  invariants on the plaquettes of the ladder. We map the model to a fermionic system and identify the topological sectors associated with different  $Z_2$  patterns in terms of fermion occupation numbers. Within these different sectors, we investigate the effect of a linear quench across a quantum critical point. We study the dominant behavior of the system by employing a Landau-Zener-type analysis of the effective Hamiltonian in the low-energy subspace for which the effective quenching can sometimes be non-linear. We show that the quenching leads to a residual energy which scales as a power of the quenching rate, and that the power depends on the topological sectors and their symmetry properties in a non-trivial way. This behavior is consistent with the general theory of quantum quenching, but with the correlation length exponent  $\nu$  being different in different sectors.

Of late, two different concepts have instigated a surge of active research in quantum many-body phenomena - the notion of topological order [1–4] and quenching across quantum critical points (QCPs) [5–9]. The former, described by global invariants, has been keenly studied for its fundamental significance, realizations in physical systems, associated phase transitions and potential applications to quantum computation. The latter has offered a mine of valuable information on the nature of the QCP in question, for instance, in the scaling behaviors of the defect density and the residual energy upon quenching. These quantities are governed by a quantum version of the Kibble-Zurek mechanism and in  $d$  dimensions, they scale with the quenching rate  $1/\tau$  as  $1/\tau^{d\nu/(z\nu+1)}$ , where  $\nu$  and  $z$  are respectively the correlation length and dynamical critical exponents of the QCP. Post-quench dynamics is thus effectual in extracting a combination of these exponents defined by the growth of the correlation length as  $|\lambda - \lambda_c|^{-\nu}$  and the relaxation time as  $|\lambda - \lambda_c|^{-z\nu}$ , as a parameter  $\lambda$  in the Hamiltonian of the system approaches a critical value  $\lambda_c$  [5, 6]. In this Letter, we demonstrate that a marriage between these two concepts makes for a synergistic union. Specifically, we show that invariants in a system having topological order can impose dramatic constraints on statics and dynamics, giving rise to quali-

tatively different post-quench behaviors; hence, quenching can act as a powerful means of discerning patterns and symmetries in the topological invariants of a system.

Our focus here is on models sharing traits of the celebrated Kitaev model [3], namely spin-1/2 lattice systems with an exponentially large number of configurations distinguished by conserved  $Z_2$  quantum numbers, which we refer to as topological sectors. Detailed studies characterizing the various topological sectors and distinguishing their physical effects are sparse; here we address these issues in the context of quenching in a simple two-legged ladder model which captures salient features of the two-dimensional parent Kitaev system. We explicitly characterize the  $Z_2$  patterns based on their periodicity and, within these different sectors, study quenching at zero temperature through a QCP. We find that the residual energy, the difference between the post-quench energy expectation value and the true ground state energy, respects the  $d\nu/(z\nu+1)$  power-law scaling form with respect to the quench rate. While the dynamical exponent takes the value  $z=1$ , the value of  $\nu$ , and therefore the power-law, depends on the topological sector being probed. For sectors endowed with higher symmetry in their periodicity,  $\nu$  deviates from unity and the power-law is no longer of the  $1/\tau^{1/2}$  form typical of many one-dimensional systems

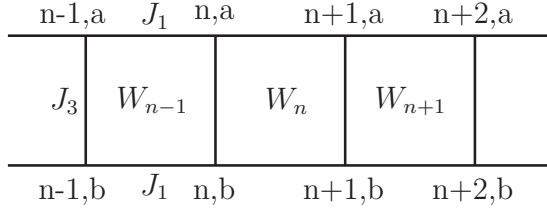


Fig. 1: Picture of the two-legged Kitaev ladder showing the couplings  $J_i$  and the  $Z_2$ -valued operators  $W_n$ .

[5, 6]. We thus theoretically demonstrate, using a simple model, the effect of topology on quantum critical behavior and the rich resultant physics in quench dynamics.

The quasi-one-dimensional Kitaev model that we consider here (see Fig. 1) consists of a two-legged ladder with a spin-1/2 at each site. We label the sites as  $(n, a)$  and  $(n, b)$ , where  $a, b$  denote the upper and lower legs respectively. The Hamiltonian for the system is given by

$$H = \sum_n [J_1(\sigma_{n,a}^x \sigma_{n+1,a}^y + \sigma_{n,b}^x \sigma_{n+1,b}^y) + J_3 \sigma_{n,a}^z \sigma_{n,b}^z], \quad (1)$$

where  $\sigma_{n,a/b}^\alpha$  denote the Pauli matrices; the couplings considered here are analogous to those associated with a strip of the honeycomb lattice in the parent Kitaev model. (We set  $\hbar = 1$ .) We assume  $J_1 > 0$ ; negative  $J_1$  values can be gauged away by performing  $\pi$ -rotations of appropriate spin components. As discussed in Ref. [10], the system exhibits a rich phase diagram as a function of the couplings  $J_1$  and  $J_3$ . Each plaquette of the ladder hosts a topological invariant and together these invariants characterize different topological sectors. For a given plaquette (see Fig. 1), we can define a Hermitian operator  $W_n = \sigma_{n,a}^y \sigma_{n,b}^y \sigma_{n+1,a}^x \sigma_{n+1,b}^x$ . One can show that the  $W_n$ 's commute with each other and with the Hamiltonian, and that  $W_n^2 = 1$ . The invariant eigenvalues,  $W_n = \pm 1$ , provide a set of  $Z_2$  quantum numbers and, for a system with  $N$  plaquettes, yield  $2^N$  distinct sectors corresponding to different sets of these numbers.

As in previous studies [10, 11], we map the system to that of two sets of spinless fermions, one probing the dynamics and the other associated with the Kitaev model's hallmark Ising anyons [1]. The mapping involves a Jordan-Wigner transformation which takes the form  $a_n = S_{n,a} \sigma_{n,a}^y$ ,  $c_n = S_{n,a} \sigma_{n,a}^x$ ,  $b_n = S_{n,b} \sigma_{n,b}^y$ ,  $d_n = S_{n,b} \sigma_{n,b}^x$ , where  $S_{n,a/b}$  denote a string of  $\sigma_{m,a/b}^z$ 's defined as follows. Assuming that each leg contains  $N$  sites with open (rather than periodic) boundary conditions,  $S_{n,a} = \prod_{m=1}^{n-1} \sigma_{m,a}^z$  weaves from the left to the right along the top leg in Fig. 1 to the  $(n-1)$ -th site, and  $S_{n,b} = \prod_{m=1}^N \sigma_{m,a}^z \prod_{m=n+1}^N \sigma_{m,b}^z$  weaves completely along the top leg left to right and then along the bottom leg from right to left to the  $(n+1)$ -th site. The transformed Hermitian operators are Majorana fermion operators satisfying relations such as  $a_n^2 = 1$ ,  $\{a_m, a_n\} = 2\delta_{mn}$ ,  $\{a_m, b_n\} = 0$ , and so on. The resultant Hamiltonian takes the form  $H =$

$\sum_n [-iJ_1(a_n a_{n+1} + b_n b_{n+1}) + i(-1)^n J_3 a_n b_n \prod_{m=n}^N W_m]$ , where  $W_n = -(ic_n d_n)(ic_{n+1} d_{n+1})$ . Thus, the Hamiltonian is quadratic in the  $a-b$  fermions and dependent on the  $Z_2$  values of the topological invariants.

Next, the Majorana fermions can be combined pairwise to form Dirac fermions, providing an understanding of the system in terms of Dirac fermion occupation numbers. The natural combinations, which pair partners on each rung of the ladder, are  $f_n = (i^n/2)(a_n + ib_n)$  and  $g_n = (1/2)(c_n + id_n)$ ; these satisfy  $\{f_m, f_n^\dagger\} = \{g_m, g_n^\dagger\} = \delta_{m,n}$ . The topological invariants can be expressed in terms of occupation numbers of the  $g$ -fermions ( $g_n^\dagger g_n = 0, 1$ ) as  $W_n = -s_n s_{n+1}$  where  $s_n = ic_n d_n = 2g_n^\dagger g_n - 1$ . The value of  $W$  on the  $n$ -th plaquette is  $+1$  if its bordering  $g$ -fermions have opposite occupation numbers and  $-1$  if they are the same. The  $s_n$ 's themselves are non-local in terms of the  $W_n$ 's:  $s_n = \prod_{m=n}^\infty W_m$ . Specifying the values  $s_n = \pm 1$  completely fixes those of the  $W_n$ 's. For instance, alternating values of  $s_n$  along the ladder gives all  $W_n = +1$ , a constant value of  $s_n$  gives all  $W_n = -1$ , and a domain wall in  $s_n$  is equivalent to embedding a  $W_n = +1$  at the wall amidst all other  $W_n$ 's being  $-1$ . [Changing the values of  $W_n$  and thus the topological sector can be achieved by the appropriate local action of operators such as  $\sigma_{n,a}^y \sigma_{n+1,a}^x$  and  $\sigma_{n,b}^y \sigma_{n+1,b}^x$ , which can alter the occupation numbers of the  $g$ -fermions on any given site]. In the thermodynamic limit, the Hamiltonian in Eq. (1) takes the local form

$$H = \sum_n [-2J_1(f_{n+1}^\dagger f_n + f_n^\dagger f_{n+1}) + J_3 s_n (2f_n^\dagger f_n - 1)], \quad (2)$$

namely a tight-binding system for the  $f$ -fermions whose on-site chemical potential is determined by the  $g$ -fermion occupation number. The Hilbert space of  $2^{2N}$  associated with the  $2N$  spins on a  $N$ -plaquette ladder is thus split into two Hilbert spaces, each of dimension  $2^N$ , corresponding to those of the 'dual'  $f$  and  $g$  fermions (whose roles can be exchanged by swapping the  $x$  and  $y$  spin components.) The  $f$ -fermions probe the dynamics of the system, while the  $g$ -fermions, whose Hilbert space dimension reflects the  $SU(2)_2$  structure associated with Ising anyons [1], determine its topology.

The topological sectors for this model can be identified by the patterns exhibited by the  $s_n$ 's. For patterns of  $s_n$  having a period  $p$ , the Hamiltonian of Eq. (2) splits up into decoupled sub-systems involving  $p$  momentum states with values  $k + 2\pi q/p$ , where  $q$  is an integer satisfying  $0 \leq q \leq p-1$  and  $k$  lies in the range  $-\pi < k \leq -\pi + 2\pi/p$ . To determine the filling of the  $f$ -fermions for the lowest energy state within a given sector, consider the limit  $J_1 = 0$  and  $J_3 < 0$ . Here energy minimization requires that the occupation number  $f_n^\dagger f_n$  at site  $n$  be equal to  $(1 + s_n)/2$ ; the gap to the first excited state is given by  $2|J_3|$ . A periodicity having  $m$  of the  $s_n$ 's be  $+1$  and  $p-m$  be  $-1$  thus has  $m$  sites occupied and the others unoccupied within a period; the filling is  $m/p$ . Turning on  $J_1$  does not change the particle number; hence the filling remains

constant in the lowest energy state. As can be shown perturbatively around the  $J_1 = 0$  limit, a small value of  $J_1$  changes the ground state energy, to second-order in  $J_1$ , by  $\Delta E_0 = -(J_1^2/J_3) \sum_n (1 - s_n s_{n+1})$ . Hence, the ground state sector in which the energy of the lowest-lying state is the minimum amidst all the sectors is the one in which  $s_n = (-1)^n$  and  $W_n = 1$  for all  $n$ .

Having characterized the system by the different topological sectors and their eigenstate structures, we now investigate the effects of quenching within different topological sectors. We assume that the system is initially placed in a particular sector; a key feature of a topological sector is that the system will remain in that sector at all times if there are no perturbations which can dynamically change the topological invariants. We initialize the system in its lowest energy state at  $J_3 = -\infty$ ; at that point, the energy gap between the ground state and the excited states is infinitely large. We then vary  $J_3$  linearly in time as  $J_3(t) = J_1 t / \tau$ ; this quench tunes the system through a QCP at  $J_3 = 0$  as discussed below. We quantify the effect of the quench via the residual energy per site attained at the final time, which is defined as

$$E_r = \lim_{t, N \rightarrow \infty} \frac{\langle H \rangle_f - E_0}{N |J_3(t)|}, \quad (3)$$

where  $\langle H \rangle_f$  denotes the expectation value of the Hamiltonian in the final state reached, and  $E_0$  is the ground state energy at  $t \rightarrow \infty$ . We study the dependence of  $E_r$  on  $\tau$  for  $J_1 \tau \gg 1$ ; this must vanish in the adiabatic limit  $\tau \rightarrow \infty$ . We find that  $E_r$  shows different qualitative trends depending on the manner in which the topologically sensitive  $J_3$  term in Eq. (2) couples different momentum modes. We discuss three distinct classes of behavior: (i) the trivial case of decoupled modes, (ii) a Landau-Zener type  $\tau^{-1/2}$  dependence of  $E_r$  due to direct coupling between the low-energy modes, and (iii) the most interesting case of a non-trivial power-law due to an indirect coupling.

Let us represent the  $f$ -fermions in the momentum basis as  $\tilde{f}_k = \frac{1}{\sqrt{N}} \sum_n f_n e^{-ikn}$ , where  $-\pi < k \leq \pi$ . In this basis, the sector having all  $W_n = -1$ , i.e., all  $s_n = 1$  for all  $n$ , can be seen to behave trivially under quenching. The modes having different momenta do not mix for any  $J_3$  in the Hamiltonian of Eq. (2). Thus, if one begins in the lowest energy state for  $J_3 = -\infty$ , i.e., with  $f_n^\dagger f_n = 1$ , one remains in that state as  $J_3$  changes to  $\infty$  where it becomes the highest excited state. Hence, the residual energy  $E_r$  is equal to 2 independently of the value of  $\tau$ .

The ground state sector having all  $W_n = 1$  offers an instance of direct coupling between low-energy modes. Assuming that  $s_n = (-1)^n$ , the Hamiltonian decouples into sub-systems having pairs of momenta  $k$  and  $k + \pi$  as

$$H_2 = \sum_k \vec{f}_{k2}^\dagger \begin{pmatrix} 4J_1 \cos k & 2J_3 \\ 2J_3 & -4J_1 \cos k \end{pmatrix} \vec{f}_{k2}, \quad (4)$$

where  $\vec{f}_{k2} = (\tilde{f}_{k+\pi}, \tilde{f}_k)^T$  represents the momentum mode annihilation operators ( $T$  denotes the transpose), and

$-\pi < k \leq 0$ . The corresponding eigenenergies are  $E_{k\pm} = \pm \sqrt{4J_3^2 + 16J_1^2 \cos^2 k}$ . For  $J_3 = 0$ , the energies vanish at  $k = -\pi/2$ , indicative of a quantum critical point (QCP); in fact, a QCP having gapless modes at  $k_c = \pm\pi/2$  occurs at  $J_3 = 0$  in any topological sector with a half-filled ground state. Here, the dynamical critical exponent is  $z = 1$  and the correlation length exponent is  $\nu = 1$  since the energy vanishes as  $|k - k_c|$  at the QCP at  $J_3 = 0$  and as  $|J_3|$  at  $k = k_c$ .

For the quench  $J_3 = J_1 t / \tau$ , a  $\pi/2$  unitary rotation interchanges the diagonal and off-diagonal terms in the matrix appearing in Eq. (4), exactly mapping the quench to the well-known Landau-Zener problem [6, 7, 12]. The probability  $p_k$  of ending in an excited state at  $t \rightarrow \infty$  and the net residual energy, for which each sub-system contributes  $4p_k$ , are therefore given by

$$p_k = \exp[-8\pi\tau J_1 \cos^2 k], \quad E_r = \int_{-\pi}^0 \frac{dk}{2\pi} 4p_k. \quad (5)$$

The probability  $p_k$  is largest for the low-energy modes near  $k_c = -\pi/2$  since this is where the gap between the two states vanishes for  $J_3 = 0$ . In the limit  $\tau J_1 \rightarrow \infty$ , the residual energy is dominated by this low-energy regime; expanding around  $k_c$  yields a Gaussian integral and the power-law form  $E_r \sim 1/\tau^{1/2}$ . This scaling is consistent with the values of the critical exponents given above and in keeping with quenches through QCPs in many one-dimensional systems [5, 6].

We now turn to an instance of a topological sector yielding a completely different quench power-law of  $1/\tau^{2/3}$  due to a higher symmetry in its periodic structure, as we show by heuristic arguments and numerics. The instance is of  $W_n = (-1)^n$ , or equivalently, the signs of  $s_n$  forming the half-filling period 4 pattern  $(++--)$ . The pattern can be expressed as  $s_n = -\sqrt{2} \cos(\pi n/2 + \pi/4)$ . The resulting Hamiltonian of Eq. (2) decouples into sub-systems involving four momenta with annihilation operators  $\vec{f}_{k4} = (\tilde{f}_{k+3\pi/2}, \tilde{f}_{k+\pi}, \tilde{f}_{k+\pi/2}, \tilde{f}_k)^T$ , where  $k$  lies in the range  $-\pi < k \leq -\pi/2$ . Explicitly,  $H_4 = \sum_k \vec{f}_{k4}^\dagger H_{k4} \vec{f}_{k4}$ , where  $H_{k4} = M_k + N_k$  with

$$M_k = -J_3 \sqrt{2} \left[ \begin{pmatrix} 0 & \beta \\ \beta^* & 0 \end{pmatrix} \otimes I + \begin{pmatrix} 0 & \beta^* \\ \beta & 0 \end{pmatrix} \otimes \mu^x \right] \quad (6)$$

$$N_k = 4J_1 \begin{pmatrix} -\sin k & 0 \\ 0 & \cos k \end{pmatrix} \otimes \mu^z. \quad (7)$$

Here  $\beta = e^{i\pi/4}$ ,  $\mu^\alpha$  denote Pauli matrices and  $I$  is the identity matrix. The higher symmetry of this sector is reflected by the fact that while the four momentum states cannot be decoupled into pairs, they are not all directly coupled to one another. The eigenenergies of  $H_{k4}$  come in pairs  $\pm E_{k4}$ , as can be derived from the symmetry property  $U H_{k4} U^\dagger = -H_{k4}$ , where  $U = \mu^z \otimes \mu^x$ . The QCP associated with this system occurs, as reflected in Eqs. (6-7), at  $J_3 = 0$  and  $k$  close to  $-\pi$  and  $-\pi/2$ . For a quench  $J_3 = J_1 t / \tau$ , the dominant contribution to the residual

energy comes from particle-hole pairs closest to the Fermi level at zero energy for which the cost of quenching into an excited state is low. For instance, for momenta  $k \gtrsim -\pi$ , the relevant pairs closest to the Fermi energy at small  $J_3$  are  $|1, 0\rangle$  and  $|0, 1\rangle$ , where  $n_p$  and  $n_0$  in state  $|n_p, n_0\rangle$  denote  $f$ -fermion occupation numbers of momenta  $k$  and  $k+\pi$ , respectively. These states are not directly coupled by the Hamiltonian  $H_{k4}$  and only mix via the higher energy states at  $k+\pi/2$  and  $k+3\pi/2$ . To second-order perturbation in  $J_3$ , this coupling is of order  $J_3^2/J_1$ ; the effective Hamiltonian for the two-level system, in the appropriate basis, takes the form

$$H_{k4,eff} = J_1 \begin{pmatrix} t^2/\tau^2 & 4k \\ 4k & -t^2/\tau^2 \end{pmatrix}, \quad (8)$$

where we have expanded  $-\sin(k-\pi) \simeq k$ , and have used the time-dependent form of  $J_3 = J_1 t/\tau$ . A similar form applies to modes at  $k \lesssim -\pi/2$ . Arguments similar to the previous case show that here  $z = 1$  and  $\nu = 2$ .

The effective quench in Eq. (8) is quadratic in time. Unlike the linear quenching problem, no exact solution is known for the excitation probability  $p_k$  for the Schrödinger equation  $id\psi_k/dt = H_{k4,eff}\psi_k$  given by Eq. (8). However, we can invoke scaling arguments to find the power-law dependence of  $p_k$  on  $\tau$ . Rescaling time as  $t' = t/\tau^{2/3}$  results in the excitation probability being governed by the parameter  $k\tau^{2/3}$ . If  $k\tau^{2/3} \lesssim 1$ , the corresponding modes have a significant weight for occupying the excited state as  $t' \rightarrow \infty$ , while the modes with  $k\tau^{2/3} \gg 1$  remain in the ground state. Integrating  $p_k$  around the low-energy modes to obtain the residual energy thus results in the scaling  $E_r \sim 1/\tau^{2/3}$ . We ascertain this behavior by numerically solving the time-dependent Schrödinger equation given by the full-fledged Hamiltonian in Eqs. (6-7) from  $t = -\infty$  to  $\infty$  with  $J_3 = J_1 t/\tau$ . We start in the lowest energy state at  $J_3 = -\infty$  consisting of the two occupied states  $(1, -1, 1, -1)/2$  and  $(1, i, -1, -i)/2$ , and time evolve to obtain the probability  $p_k$  for occupying the excited states. The left panel of Fig. 2 shows the resultant  $p_k$  versus the scaled variable  $(k+\pi)(J_1\tau)^{2/3}$  for  $k \gtrsim -\pi$ ; the curve is independent of  $\tau$  for  $J_1\tau \gg 1$ . The probability  $p_k$  near  $k \lesssim -\pi/2$  is related to this curve by mirror symmetry. Analogous to Eq. (5), integrating  $2p_k/\pi$  over  $k$  from  $-\pi$  to  $-\pi/2$  yields the residual energy  $E_r$ . The right panel of Fig. 2 shows a plot of  $\log(E_r)$  versus  $\log(J_1\tau)$ . The clean linear fit with a slope close to  $-2/3$  confirms our predicted  $1/\tau^{2/3}$  scaling form.

This unusual power-law scaling is generic to a series of topological sectors that are at half-filling, i.e., those that in a period  $2m$  have half the  $s_n$ 's take on the value  $+1$ . Of the associated  $2m$  momentum modes, the states closest to  $k = \pm\pi/2$  and thus to the Fermi energy dominate the quench. As in the example above, the quench through the QCP at  $J_3 = 0$  shows unusual scaling if these states are not directly coupled. This corresponds to the  $J_3$  term in the Hamiltonian having no matrix element between the low-energy modes or, equivalently, having  $A_m$  vanish in

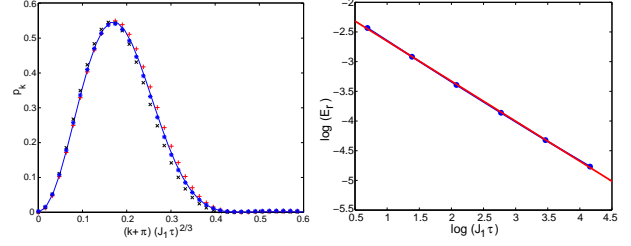


Fig. 2: Left panel: Plot of  $p_k$  versus  $(k+\pi)(J_1\tau)^{2/3}$  for  $k \gtrsim -\pi$ , and  $J_1\tau = 2$  (red +), 8 (black x) and 32 (blue \*). Right panel: Logarithmic plot of  $E_r$  versus  $J_1\tau$  in the sector with  $W_n = (-1)^n$ . A linear fit gives  $E_r = 0.14/(J_1\tau)^{0.67}$  which is close to a  $-2/3$  power-law.

the Fourier expansion  $A_l = \sum_{j=1}^{2m} s_j e^{i\pi j l/m}$ . Clearly the number of such cases increases with increasing  $m$ . For instance, such examples of period 8 which also yield the  $1/\tau^{2/3}$  power-law by way of low-energy modes being coupled via one intermediate high energy state are the sets  $(++++----)$ ,  $(+++--+--)$ ,  $(++-++--)$ ,  $(+-+--+--)$ , and cyclic permutations thereof. However, in cases of even higher symmetry where the low-energy modes are only coupled via a path involving  $q$  intermediate high energy states, the effective coupling is of the form  $J_1(t/\tau)^{q+1}$  for the linear quench  $J_3 = J_1 t/\tau$ . In principle, the generalized scaling argument presented above would predict that the residual energy would have the scaling form  $E_r \sim \tau^{-(q+1)/(q+2)}$  corresponding to  $z = 1$  and  $\nu = q+1$ , but the analysis would depend on the specific topological sector and dominant couplings close to the QCP.

In conclusion, we have demonstrated that in certain systems, topological order can play a major role in determining the universality class and behavior close to QCPs. Topology can greatly constrain dynamics and yield unusual power-law scaling in quenches across QCPs which can distinguish different orderings based on symmetry properties. The one-dimensional example showcased here ought to be realizable using recent schemes proposed in cold atomic systems [13] and the associated topological sectors ought to be accessed using local operations. We expect that topology-driven scaling forms would be manifest in several observables such as dynamic spin-spin correlations, and in two-dimensional generalizations of the Kitaev model. Finally, due to a finite quantum critical regime in parameter space and the robustness of topological sectors against a large class of perturbations, we expect the features discussed here to persist at temperatures much smaller than the energy gap at the initial time. At higher temperatures, the interplay between thermal and quantum fluctuations on quench dynamics [14] would require further investigation in our model.

We thank K. Sengupta, S. Deng and S. Trebst for illuminating discussions. We gratefully acknowledge the support of DST, India under Project No. SR/S2/CMP-27/2006



(DS), the NSF under the grant DMR 06-44022 CAR (SV) and the CAS fellowship at UIUC (SV).

## REFERENCES

- [1] C. Nayak, S. H. Simon, A. Stern, M. Freedman and S. Das Sarma, *Rev. Mod. Phys.*, **80** (2008) 1083, and references therein.
- [2] M. A. Levin and X.-G. Wen, *Phys. Rev. B*, **71** (2005) 045110.
- [3] A. Kitaev, *Ann. Phys. (N.Y.)*, **321** (2006) 2.
- [4] S. Das Sarma, M. Freedman and C. Nayak, *Physics Today*, **59**, issue No. 7 (2006) 32.
- [5] T. W. B. Kibble, *J. Phys. A*, **9** (1976) 1387, and *Phys. Rep.*, **67** (1980) 183; W. H. Zurek, *Nature (London)*, **317** (1985) 505, and *Phys. Rep.*, **276** (1996) 177.
- [6] W. H. Zurek, U. Dörner and P. Zoller, *Phys. Rev. Lett.*, **95** (2005) 105701; J. Dziarmaga, *Phys. Rev. Lett.*, **95** (2005) 245701; B. Damski, *Phys. Rev. Lett.*, **95** (2005) 035701; A. Polkovnikov, *Phys. Rev. B*, **72** (2005) 161201(R); A. Polkovnikov and V. Gritsev, *Nature Phys.*, **4** (2008) 477.
- [7] R. W. Cherng and L. S. Levitov, *Phys. Rev. A*, **73** (2006) 043614; V. Mukherjee, U. Divakaran, A. Dutta and D. Sen, *Phys. Rev. B*, **76** (2007) 174303; U. Divakaran, A. Dutta and D. Sen, *Phys. Rev. B*, **78** (2008) 144301; S. Deng, G. Ortiz and L. Viola, *EPL*, **84** (2008) 67008; U. Divakaran, V. Mukherjee, A. Dutta and D. Sen, *J. Stat. Mech: Theory Exp.*, P02007 (2009).
- [8] K. Sengupta, D. Sen and S. Mondal, *Phys. Rev. Lett.*, **100** (2008) 077204; S. Mondal, D. Sen and K. Sengupta, *Phys. Rev. B*, **78** (2008) 045101; D. Sen, K. Sengupta and S. Mondal, *Phys. Rev. Lett.*, **101** (2008) 016806; S. Mondal, K. Sengupta and D. Sen, *Phys. Rev. B*, **79** (2009) 045128; R. Barankov and A. Polkovnikov, *Phys. Rev. Lett.*, **101** (2008) 076801; C. De Grandi, V. Gritsev and A. Polkovnikov, *Phys. Rev. B*, **81** (2010) 012303.
- [9] J. Dziarmaga, arXiv:0912.4034.
- [10] X.-Y. Feng, G.-M. Zhang and T. Xiang, *Phys. Rev. Lett.*, **98** (2007) 087204.
- [11] H.-D. Chen and Z. Nussinov, *J. Phys. A*, **41** (2008) 075001; Z. Nussinov and G. Ortiz, *Phys. Rev. B*, **77** (2008) 064302; G. Baskaran, S. Mandal and R. Shankar, *Phys. Rev. Lett.*, **98** (2007) 247201; K. P. Schmidt, S. Dusuel and J. Vidal, *Phys. Rev. Lett.*, **100** (2008) 057208; D.-H. Lee, G.-M. Zhang and T. Xiang, *Phys. Rev. Lett.*, **99** (2007) 196805.
- [12] C. Zener, *Proc. Roy. Soc. London, Ser. A*, **137** (1932) 696; L. Landau and E. M. Lifshitz, *Quantum Mechanics: Non-relativistic Theory*, 2nd Ed. (Pergamon Press, Oxford, 1965).
- [13] L.-M. Duan, E. Demler and M. D. Lukin, *Phys. Rev. Lett.*, **91** (2003) 090402; A. Micheli, G. K. Brennen and P. Zoller, *Nature Phys.*, **2** (2006) 341.
- [14] D. Patanè, A. Silva, L. Amico, R. Fazio and G. E. Santoro, *Phys. Rev. Lett.*, **101** (2008) 175701.